INEEL/CON-04-02512
PREPRINT

Oxidation Behavior Of In-Flight Molten Aluminum Droplets In The Twin-Wire Electric Arc Thermal Spray Process

Donna Post Guillen
Brian G. Williams

May 2-4, 2005

2005 International Thermal Spray Conference

Oxidation Behavior of In-Flight Molten Aluminum Droplets in the Twin-Wire Electric Arc Thermal Spray Process

Donna Post Guillen, Idaho National Engineering and Environmental Laboratory, Idaho Falls, Idaho, USA
Brian G. Williams, Idaho State University, Pocatello, Idaho, USA

This paper examines the in-flight oxidation of molten aluminum sprayed in air using the twin-wire electric arc (TWEA) thermal spray process. The oxidation reaction of aluminum in air is highly exothermic and is represented by a heat generation term in the energy balance. Aerodynamic shear at the droplet surface: (1) enhances the amount of in-flight oxidation by promoting entrainment and mixing of the surface oxides within the droplet, and (2) causes a continuous heat generation effect due to the exothermic oxidation reaction that sustains droplet temperature as compared to a droplet without internal circulation. This continual source of heat input keeps the droplets in a liquid state during flight. A linear rate law based on the Mott-Cabrera theory was used to estimate the growth of the surface oxide layer formed during droplet flight. An explanation is provided for the elevated, nearly constant surface temperature (~ 2000 °C) of the droplets during flight to the substrate and it is shown that the majority of oxide content in the coating is produced during flight, rather than after deposition. The calculated oxide volume fraction of an average droplet at impact agrees well with the experimentally determined oxide content for a typical TWEA-sprayed aluminum coating, which ranges from 3.3 to 12.7%.

1 Introduction

This paper analyzes the oxidation behavior of an average in-flight molten aluminum droplet produced by the twin-wire electric arc (TWEA) thermal spray process. Measurements of droplet size, velocity, and temperature in the spray plume obtained by Hale, et al. [1] using in-flight particle pyrometry and laser Doppler velocimetry were the basis for the estimating fluid and thermal effects. In addition, pitot tube measurements provided information on the velocity of the freestream air, which enabled the relative velocity between the droplets and the ambient air to be calculated. The fluid dynamic effects cause a toroidal flow within the droplet that enhances oxidation, resulting in an elevated temperature during droplet flight to the substrate and an increase in the final oxidation percentage of a typical coating, as compared to a droplet without internal circulation. The results from this analysis correlate with the experimental data for in-flight droplet temperature [1] and for coating oxide content [2].

2 Aluminum Oxidation Reaction

Aluminum is a reactive metal with a strong affinity for oxygen [3]. The oxidation of aluminum in air is governed by the following equation [4]:

$$2Al + 1.5O_2 = Al_2O_3 - 1675.7 \text{ kJ}.$$

The reaction is highly exothermic, and the small droplet sizes offer a large surface area to volume ratio available for oxidation. In this paper, it will be shown that high droplet temperatures are sustained due to the continuous oxidation reaction. Inflight particle pyrometry data shows that the centerline droplet temperature remains fairly constant (around 2000 °C) during droplet flight [1]. At this temperature, the droplets are in a liquid state. In-flight oxidation of the aluminum droplets is accompanied by two effects: (1) a fluid dynamic effect, which promotes entrainment and mixing of the surface oxides within the droplet, and (2) a heat transfer effect due to the exothermic oxidation reaction, which causes an increase in droplet temperature over that of a rigid sphere (i.e., a droplet without internal circulation).

3 Fluid Dynamic Effect

It is well known that aerodynamic shear induces internal circulation in droplets, such as fuel sprays and raindrops [5]. The resulting convective effect within a liquid droplet, also known as Hill's spherical vortex, was described over a century ago [6]. LeClair et al. [7] observed flow patterns within a water droplet falling at terminal velocity in air by experiments performed in a wind tunnel where the water droplets were seeded with carbon or aluminum tracer particles and the internal circulation was recorded using streak photography. More recently, Melton [8] has used droplet exciplex (e.g., excited complex) fluorescence to experimentally verify internal circulation in liquid droplets. The existence of such phenomena in droplets produced by thermal spray processes was suggested by Neiser, et al. [9]. The presence of a two-dimensional toroidal flow field within the molten droplets is stimulated by shear forces due to the high-velocity gas flow around the droplets, **Figure 1**.

This liquid motion continually sweeps fresh fluid to the surface of the droplet where it is available for oxidation. The oxide that forms at the droplet surface is entrained into the particle and mixed with the liquid aluminum by convective motion within the droplet. The internal circulation of the in-flight molten aluminum droplets in the TWEA spray process affects the amount of oxides in the droplets, and as a result, the as-sprayed coating.

Using the experimental data produced by Hale, et al. [1], a 39 μm aluminum droplet traveling through ambient air (T_∞=25 °C) at a relative velocity of 140 m/s with a constant temperature of 2000 °C was used to represent a "typical" droplet in the spray plume. By scaling the data generated by LeClair et al. [7] to the correct viscosity ratio, relative velocity, and Reynolds number for the liquid aluminum/air system, an average internal circulation velocity, $\bar{v}$, of 8.4 m/s is obtained for this "typical" droplet. The relative velocity between the droplets and the air in the spray plume is depicted in **Figure 2.**

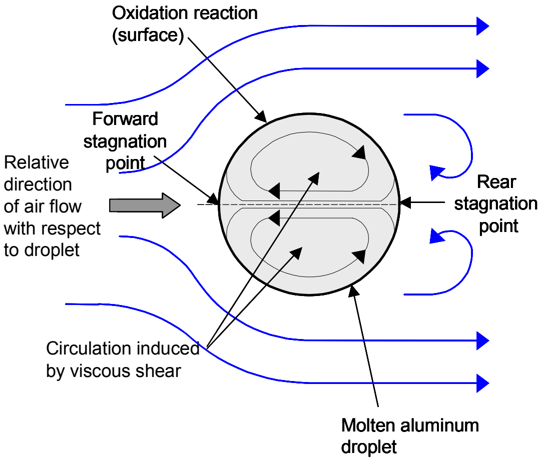

Figure 1. Internal circulation within a fully molten droplet caused by shear forces from the high-velocity airflow around the droplet.

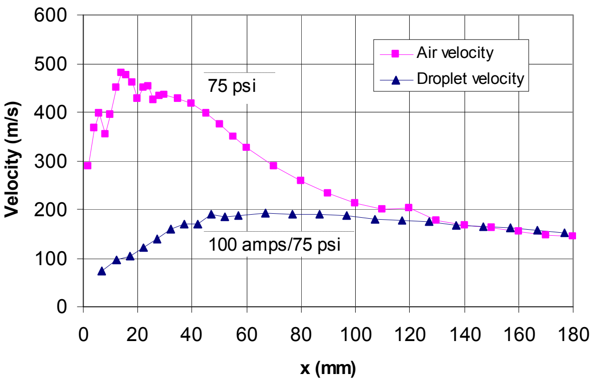

Figure 2. Comparison of droplet and air velocities along spray plume centerline [1].

4 Heat Generation Effect

The energy balance at the surface of the in-flight droplet is given by the following equation representing conservation of energy for a control volume:

$$\dot{E}_g - \dot{E}_{out} = \dot{E}_{st} \qquad (1)$$

where $\dot{E}_g$ is the rate of energy generation within the control volume, $\dot{E}_{out}$ is the rate of energy leaving the system through the control volume, and $\dot{E}_{st}$ is the rate of energy storage within the control volume.

Neglecting the latent heat release due to the solidification of aluminum oxide particles, the energy generation term can be represented as

$$\dot{E}_g = \dot{m}H_f$$

where H_f is the heat of formation of aluminum oxide, and the mass flow rate supplied to the oxidation reaction due to internal circulation, $\dot{m}$, can be represented as

$$\dot{m} = \int \rho_{Al} \frac{d\delta}{dt} \cdot dA_{ox} \qquad (2)$$

In Equation 2, ρ_{Al} is the density of molten aluminum, $\frac{d\delta}{dt}$ is the rate of growth of the oxide layer, and dA_{ox} is the incremental oxidation area of the spherical droplet. A linear rate law based on the Mott-Cabrera theory was used to estimate the rate of growth of the surface oxide layer during droplet flight [10; 11]:

$$\frac{d\delta}{dt} = 2A_0 \exp\left(-\frac{Q}{k_b T_d}\right) \exp\left(k_e \frac{P_{O_2}^{\frac{1}{2}}}{k_b T_d}\right) \qquad (3)$$

where the oxidation equation constants for aluminum are given by Dai et al. [10] as

$A_0=2.5(10)^6$ Å/s
Q=1.6 eV
k_e=0.139 eV/torr
k_b (Boltzman constant)=$1.38(10)^{-23}$ J/K

and the experimental conditions yielded a droplet temperature, T_d, of 2273K and an oxygen partial pressure, P_{O2}, of 134 torr (at a laboratory altitude of 1371.6 m above sea level).

An expression for the oxidation area as a function of droplet radius, R, and average internal circulation velocity can be obtained. The droplet surface area that oxidizes is that of a spherical cap [12]

$$dA_{ox} = 2\pi R \int_0^h dh \qquad (4)$$

where h is the length of the spherical cap, as shown in **Figure 3**.

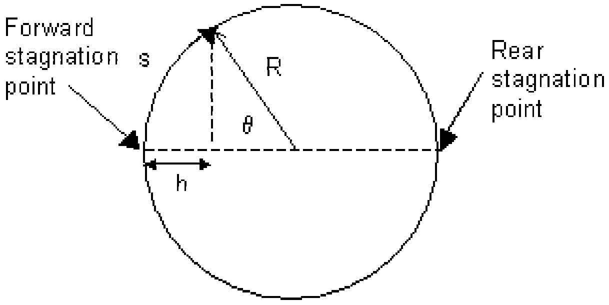

Figure 3. Graphical representation of spherical cap oxidation area.

From geometry,

$$h=R(1-\cos\theta)$$

and

$$\theta=\frac{s}{R} \text{ and } s=\bar{v}t$$

where s is the wetted length along the droplet surface.

Integrating Equation 4 yields

$$\left\{\begin{array}{l} A_{ox}=2\pi R^2\left(1-\cos\left(\frac{\bar{v}t}{R}\right)\right) \text{ for } t<t_{cycle} \\ \\ A_{ox}=A=4\pi R^2 \text{ for } t>t_{cycle} \end{array}\right\}$$

where A is the surface area of a sphere and t_{cycle} is the time for one circulation cycle. A circulation cycle is defined here as the time for an oxide particle to travel from the forward stagnation point along the droplet surface to the rear stagnation point of the droplet.

Using this information, the energy generation rate for a “typical” droplet due to the oxidation reaction is calculated to be $\dot{E}_g=0.088$ W.

Newton’s law of cooling is used to estimate the heat convected from the molten droplet [13] by the equation

$$\dot{E}_{out}=h_{conv}A(T_d-T_\infty).$$

Using the Ranz Marshall correlation evaluated at the film temperature [14], the convection heat transfer coefficient, h_{conv}, is calculated to be 10345 W/ $m^2 \cdot K$ yielding $\dot{E}_{out}$ equal to 0.098 W. The heat loss from the system due to radiation is negligible compared to the convective loss. The rate of energy storage within the control volume is given by

$$\dot{E}_{st}=\rho_{Al}c_p\forall_d\frac{dT_d}{dt} \qquad (5)$$

where ρ_{Al} is the density of molten aluminum, c_p is the specific heat of molten aluminum, $\forall_d$ is the volume of the spherical droplet, and $\frac{dT_d}{dt}$ is the time rate of change of temperature of the droplet. Inserting Equation 5 into Equation 1 and rearranging, the rate of change of droplet temperature is given by

$$\frac{dT_d}{dt}=\frac{\dot{E}_g-\dot{E}_{out}}{\rho_{Al}c_p\forall_d} \qquad (6)$$

Since $\dot{E}_g \approx \dot{E}_{out}$,

$$\frac{dT_d}{dt}\approx 0$$

and the droplet temperature remains nearly constant, as seen in the experimental measurements.

When the rate of energy generation, $\dot{E}_g$, is neglected, the solution to Equation 6 becomes

$$T_d=T_\infty+(T_{di}-T_\infty)e^{-ct} \qquad (7)$$

where T_{di} is the initial droplet temperature and

$$c=\frac{h_{conv}A}{\rho_{Al}c_p\forall_d}=733/s$$

The Biot number for this case is «1, indicating that a lumped capacitance assumption is valid [13]. Using Equation 7 to calculate the transient droplet temperature during transport to the substrate closely approximates the computational fluid dynamic results of Varacalle et al.,1994 [15]. Varacalle et al., 1994 predicted that the temperature of a 39 μm TWEA-sprayed aluminum droplet will decrease to approximately 950 K from an initial temperature of 2373 K over a distance of 178 mm from the thermal spray gun exit. As calculated by Equation 7, without heat generation the droplet temperature would decrease to approximately 1075 K over a distance of 178 mm from an initial temperature of 2273 K. **Figure 4** compares the transient temperature profiles of the experimental measurements, Varacalle’s results, and calculations that neglect the continual heat generation term.

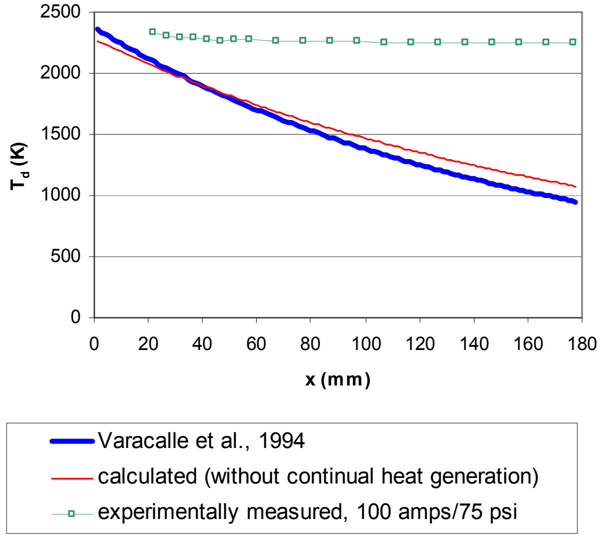

Figure 4. Comparison of droplet temperatures along spray plume centerline with and without internal heat generation.

If the energy generation term is neglected in the surface energy balance equation, the temperature of a “typical” droplet will decrease due to convective cooling as it travels to the substrate instead of remaining nearly constant, as seen in the experimental measurements. Varacalle et al., 1994 included the initial heat input from the oxidation of the molten aluminum droplets without considering the continual generation of heat produced by the oxidation reaction coupled with internal circulation within the molten droplet. The importance of including the heat generation input from the oxidation reaction as a continual source term in the energy balance is clearly demonstrated.

5 Calculation of Oxide Content

The oxide volume fraction for a rigid sphere with an oxide shell, φ_{rigid}, can be calculated by

$$\varphi_{rigid} = \frac{\not{V}_{ox}}{\not{V}_{d}}$$

where

$$\not{V}_{d} = \frac{\pi}{6} D^3 .$$

The volume of an oxide shell on the outer surface of a sphere, $\not{V}_{ox}$, is given by Shenk [16]

$$\not{V}_{ox} = \frac{\pi}{6}\left(D^3 - (D - 2\delta)^3\right)$$

From Equation 3, during one circulation cycle, a “typical” droplet will build up a surface oxide layer thickness, δ, of 39 Å.

For a droplet with internal circulation, the volume fraction, φ_{circ}, is expressed as

$$\varphi_{circ} = \frac{(\not{V}_{ox})(N)}{\not{V}_{d}}$$

where N is the number of cycles of oxide layer entrainment into the droplet. The “typical” droplet considered here will undergo 127 cycles of oxide entrainment.

Beyond a standoff distance of 130 mm, the relative velocity between the particles and the air stream goes to zero, as shown in **Figure 2**, and thus the toroidal flow inside of the droplet diminishes. Adding the oxide volume fraction due to the formation of an oxide layer on a rigid sphere (x>130 mm) to that formed by the in-flight mixing mechanism (x≤130 mm) yields an average total oxide volume fraction

$$\varphi_{tot} = \varphi_{rigid} + \varphi_{circ} = \frac{\not{V}_{ox}}{\not{V}_{d}} + \frac{(\not{V}_{ox})(N)}{\not{V}_{d}}$$

The oxide volume fraction within a droplet with internal circulation, φ_{tot}, is 0.0762 or 7.62%. The oxide content calculated for an average droplet with internal circulation correlates well with the experimentally determined oxide content in the coatings (3.3 to 12.7%) [2].

In contrast, the oxide volume fraction computed for a rigid sphere is nearly two orders of magnitude smaller than that for a droplet with internal circulation. The oxide buildup on the surface of a rigid sphere under the same flight conditions is estimated to be 0.00121 or 0.121%, which is approximately 1.5% of the oxide volume fraction for a droplet with internal circulation. This calculated value correlates well to the oxygen content of 0.116% for atomized aluminum powder [17]. The calculated oxide content for a “typical” droplet for the cases with and without internal circulation are compared to the experimentally measured oxide content in **Table 1**.

Table 1. Comparison of calculated oxide content with and without internal circulation to experimentally measured oxide content.

	Oxide content
Calculated without internal circulation	0.121%
Calculated with internal circulation	7.62 %
Experimentally measured	3.3 to 12.7%

From the Mott-Cabrera equation, the rate of growth of the oxide layer is highly sensitive to the oxygen content of the ambient air. The oxide content of the coating could be increased by performing the spraying operations at a lower altitude, where the atmospheric pressure (and thus the oxygen partial pressure) is higher. The theoretical maximum oxide content in a “typical” droplet may be calculated assuming that the oxide layer thickness reaches a maximum of 79 angstroms per circulation cycle [17]. The theoretical maximum oxide content of a “typical” droplet is, therefore, approximately 15.4%. This value is nearly double the oxide content produced at the laboratory elevation of 1371.6 m above sea level in Idaho Falls, Idaho, USA.

6 Summary and Conclusions

An explanation for the nearly constant droplet temperature measured axially along the spray plume centerline has been provided by accounting for the continual oxidation of molten aluminum due to internal circulation within the atomized droplets. Calculations of oxide content in a “typical” droplet agree with the experimentally determined oxide content in a typical thermal spray coating. The analysis performed herein shows that internal circulation within the droplet increases the oxide content of the droplet by two orders of magnitude over that of a droplet without internal circulation. Also, since the rate of aluminum oxide growth is highly sensitive to the partial pressure of oxygen in the surrounding air, the altitude at which the spraying is performed affects the amount of oxide produced in the droplet. It is important to point out that both the spray plume experiments and the coatings were fabricated at laboratories located in the same city, at approximately the same elevation. This enabled a direct comparison of the spray plume data and the coating data.

Future work will build upon the knowledge gained by comparing the experimental data to the droplet temperature predictions of Varacalle, et al. [15]. A more general equation will be developed to account for the continual heat generation produced when fresh metal is swept to the droplet surface as a result of the internal circulation within the droplet.

Acknowledgements

This work is sponsored in part by the U.S. Department of Energy under Contract Number DE-AC07-99ID13727.

References

[1] Hale, D.L., Swank, D.W., and Haggard, D.C., "In-Flight Particle Measurements of Twin Wire Electric Arc Sprayed Aluminum," *Journal of Thermal Spray Technology*, Vol. 7, No. 1, March 1998, p. 58-63.

[2] Varacalle, D.J., Jr., Mizia, R., Shelton-Davis, C., Torres, L., Zanchuck, V., and Sampson, E., "Twin-Wire Electric Arc Sprayed Zinc and Aluminum Coatings," *Proceedings of the SSPC 1996 Seminars, Technologies for a Diverse Industry*, Charlotte, NC, November 17-21, 1996, p. 137-143.

[3] Bretherick, L., *Handbook of Reactive Chemical Hazards*, 3rd ed., Butterworths, London, 1985.

[4] Wefers, K., and Misra, C., *Oxides and Hydroxides of Aluminum*, Alcoa Laboratories, 1987, p. 64.

[5] Sirignano, W.A., *Fluid Dynamics and Transport of Droplets and Sprays*, Cambridge University Press, 1999, p. 1.

[6] Hill, M.J.M. "On a spherical vortex," *Phil. Trans. R. Soc.,* Vol. 185, 1894, p. 213-245.

[7] LeClair, G.P., Hamielec, A.E., Pruppacher, H.R., and Hall, W.D., "A Theoretical and Experimental Study of the Internal Circulation in Water Drops Falling at Terminal Velocity in Air," *Journal of the Atmospheric Sciences*, Vol. 29, 1972, p. 728-740.

[8] Melton, L., "Experimental Methods for CFD Evaluation," presentation at *Computational Fluid Dynamics in Chemical Reaction Engineering VII*, Quebec, Canada, August 2000.

[9] Neiser, R.A., Smith, M.F., and Dykhuizen, R.C, "Oxidation in Wire HVOF-Sprayed Steel," *Journal of Thermal Spray Technology*, Volume 7(4), December 1998, p. 537-545.

[10] Dai, S.L., Delplanque, J.-P. Delplanque, and Lavernia, E.J., "Microstructural Characteristics of 5083 Al Alloys Processed by Reactive Spray Deposition for Net-Shape Manufacturing," *Metallurgical and Materials Transactions A*, Vol. 29A, October 1998, p. 2597-2611.

[11] Delplanque, J.-P., Lavernia, E.J., and Rangel, R.H., "Analysis of in-Flight Oxidation During Reactive Spray Atomization and Deposition Processing of Aluminum," *Transactions of the ASME*, Vol. 122, February 2000, p. 126-133.

[12] Harris, J.W. and Stocker, H., "Spherical Segment (Spherical Cap)," §4.8.4 in *Handbook of Mathematics and Computational Science*, Springer-Verlag, New York, 1998, p. 107.

[13] Incropera, F.P., and DeWitt, D.P, *Fundamentals of Heat Transfer,* John Wiley & Sons, New York, 1981.

[14] Ranz, W.E., and Marshall, W.R., Jr., "Evaporation from Drops," *Chemical Engineering Progress*, Vol. 48, No. 3, March 1952, p. 141-146.

[15] Varacalle, D.J., Jr., Wilson, G.C., Johnson, R.W., Steeper, T.J., Irons, G., Kratochvil, W.R., and Riggs, W.L., "A Taguchi Experimental Design Study of Twin-Wire Electric Arc Sprayed Aluminum Coatings," *Journal of Thermal Spray Technology*, Vol. 3, No. 1, March 1994, p. 69-74.

[16] Shenk, A., *Calculus and Analytic Geometry*, Goodyear Publishing Company, Santa Monica, CA, 1979, p. 199-200.

[17] *ASM Handbook*, Volume 2, Properties and Selection: Nonferrous Alloys and Special-Purpose Materials, ASM International, 1991.